



Original Article

Open Access



Glioma-associated oncogene (GLI)-specific decoy oligodeoxynucleotide induces apoptosis and attenuates proliferation, colony formation, and migration in liver cancer cells

Zahra Hajilou^{1,2}, Roya Solhi¹, Bahare Shokouhian¹, Shukoofeh Torabi¹, Zahra Heydari¹, Zahra Farzaneh¹, Sadaf Bahadori¹, Abbas Piryaee³, Moustapha Hassan⁴, Andreas K. Nussler⁵ , Massoud Vosough^{1,4} 

¹Department of Regenerative Medicine, Cell Science Research Center, Royan Institute for Stem Cell Biology and Technology, ACECR, Tehran 1665659911, Iran.

²Department of Developmental Biology, University of Science and Culture, Tehran 1665658822, Iran.

³Department of Biology and Anatomical Sciences, School of Medicine, Shahid Beheshti University of Medical Sciences, Tehran 1665652365, Iran.

⁴Experimental Cancer Medicine, Institution for Laboratory Medicine, Karolinska Institute, Stockholm 17177, Sweden

⁵Siegfried Weller Institute, University of Tübingen, BG Tübingen, Tübingen 72074, Germany.

Correspondence to: Dr. Massoud Vosough, Department of Regenerative Medicine, Cell Science Research Center, Royan Institute for Stem Cell Biology and Technology, ACECR, Hafez Street, Royan Avenue, Tehran 1665659911, Iran. E-mail: masvos@yahoo.com; Dr. Andreas K. Nussler, Siegfried Weller Institute, University of Tübingen, BG Tübingen, Geschwister-Scholl-Platz, Tübingen 72074, Germany. E-mail: andreas.nuessler@gmail.com

How to cite this article: Hajilou Z, Solhi R, Shokouhian B, Torabi S, Heydari Z, Farzaneh Z, Bahadori S, Piryaee A, Hassan M, Nussler AK, Vosough M. Glioma-associated oncogene (GLI)-specific decoy oligodeoxynucleotide induces apoptosis and attenuates proliferation, colony formation, and migration in liver cancer cells. *Hepatoma Res* 2024;10:32. <https://dx.doi.org/10.20517/2394-5079.2024.56>

Received: 3 Apr 2024 **First Decision:** 26 Jun 2024 **Revised:** 18 Jul 2024 **Accepted:** 24 Jul 2024 **Published:** 30 Jul 2024

Academic Editor: Giuliano Ramadori **Copy Editor:** Dong-Li Li **Production Editor:** Dong-Li Li

Abstract

Aim: Hepatocellular carcinoma (HCC) is one of the leading causes of cancer-associated death. The Sonic Hedgehog (SHH) signaling pathway participates in the initiation, progression, migration, and recurrence of HCC cancer stem cells. Furthermore, SHH regulates various cellular behaviors such as proliferation, differentiation, survival, self-renewal, epithelial-mesenchymal transition (EMT), and SHH autoregulation. Glioma-associated oncogene (GLI) family zinc finger are key transcription factors in the development of many organs and are deregulated in cancer. In this study, Huh-7 cells were treated with GLI-specific decoy oligodeoxynucleotide (ODN) to evaluate its anticancer impact.



© The Author(s) 2024. **Open Access** This article is licensed under a Creative Commons Attribution 4.0 International License (<https://creativecommons.org/licenses/by/4.0/>), which permits unrestricted use, sharing, adaptation, distribution and reproduction in any medium or format, for any purpose, even commercially, as long as you give appropriate credit to the original author(s) and the source, provide a link to the Creative Commons license, and indicate if changes were made.



Methods: The transfection efficiency of GLI-specific decoy ODN was measured using fluorescent microscopy. Then, the effects of GLI-specific decoy ODN on apoptosis, viability, proliferation rate, colony formation, and migration capacities of Huh-7 cells were assessed. Furthermore, the expression of genes associated with the alteration of SHH was assessed.

Results: Treatment of Huh-7 cells with GLI-specific decoy ODN decreased cell viability ($56.36\% \pm 3\%$). Expression of certain genes such as *c-MYC*, *SNAI2*, *ZEB1*, and *PROM1* decreased dramatically, while the expression of *CDH1* increased significantly. Furthermore, the treated cells' proliferation, colony formation, and migration capacity decreased considerably. This treatment induced apoptosis in the Huh-7 cells.

Conclusion: Inhibition of the SHH signaling pathway using GLI-specific decoy ODN led to a decline in the growth rate of HCC cells, decreased migration, and attenuated EMT progression.

Keywords: Hepatocellular carcinoma, decoy oligodeoxynucleotide, glioma-associated oncogene (GLI), sonic hedgehog signaling pathway, proliferation, colony formation, migration

INTRODUCTION

The most common and malignant type of liver cancer is hepatocellular carcinoma (HCC)^[1]. Due to the lack of early diagnosis methods, people with HCC usually face limited treatment options and poor prognosis^[2]. To effectively treat patients, surgical modalities are commonly employed as the first-line treatments for HCC, which include tumor resection and liver transplantation. Unfortunately, less than 20% of the diagnosed patients meet the criteria for surgical approaches. The recurrence rate of HCC after cross-sectional surgeries is 15%-20%, while in individuals who have undergone liver transplantation, it surges to 57%-75%^[3]. Global statistics indicate an average survival rate of five years. In terms of gender, men are more prone to liver cancer, which ranked as the second most fatal cancer worldwide for both sexes and all age groups in 2020^[4]. Inflammation and chronic liver damage are the key drivers of the development and progression of HCC^[5,6]. One of the leading causes of malignancy is the dysregulation of specific signaling pathways, which leads to aberrant changes in the expression profile of cells. Therefore, targeting the key players of irregular signaling pathways seems to be a promising therapeutic approach in cancer medicine^[7]. Notch, WNT, transforming growth factor-beta (TGF- β), receptor tyrosine kinase (RTK), and Sonic Hedgehog (SHH) signalings [Supplementary Figure 1A] are among the most critical pathways that contribute to HCC development and progression^[7,8].

The SHH pathway is naturally inactive in mature and healthy hepatocytes^[9-11]. In a healthy liver, hepatic stellate cells (HSCs) and endothelial cells produce significant Hedgehog interacting protein (HHIP). The binding of HHIP to the SHH ligand prevents it from binding to SHH-responsive target cells, thereby inhibiting the pathway^[12]. However, liver tissue damage induces the SHH pathway in hepatocytes, bile duct cells, and hepatic stellate cells. Activation of this pathway facilitates damaged liver cells' regeneration and healing process^[13].

Risk factors such as an unhealthy diet, hepatitis B and C viral infections, exposure to aflatoxin, and diseases such as non-alcoholic fatty liver disease (NAFLD) irritate liver cells^[14,15].

By inhibiting the protein patched homolog (PTCH) receptor, the SHH ligand activates the proto-oncoprotein Smoothed (SMO) receptor. The activated SMO inhibits the negative regulatory factor suppressor of fused homolog (SuFu), perpetrating the release of glioma-associated oncogene homolog (GLI) transcription factor and its translocation into the nucleus. Without the SHH ligand, PTCH inhibits SMO,

and GLIs are phosphorylated by protein kinase A (PKA)/casein kinase 1 (CK1)/glycogen synthase kinase 3 (GSK3) complex^[10,16]. After the translocation of the GLI transcription factor inside the nucleus, it binds to the promoters of target genes and regulates them^[17]. The expression of these genes plays a key role in the proliferation regulation of hepatocytes, the strengthening of liver cancer stem cells, the differentiation of these cells into lost epithelial cells, especially hepatocytes, and the regeneration of vessels^[8,9,13,18].

SHH activity is correlated to the severity of liver damage. Excessive production and secretion of SHH ligands from damaged cells such as hepatocytes, natural killer T cells, hepatic stellate cells, and activated endothelial cells induce SHH activity. The activity of the SHH pathway does not inhibit the repair process and cell death due to the reduction of caspase-9^[19].

The SHH signaling pathway facilitates cell proliferation and carcinogenesis by increasing the expression of cyclin B1 and cyclin-dependent kinase 1 (CDK1) proteins^[3,13]. Different studies have shown that in HCC cells, unlike healthy hepatocytes, genes related to pathway components such as SHH, PTCH, GLI, and SMO are abnormally overexpressed. This increased expression causes HCC tumor growth^[3,20,21]. Following the activation of the SHH pathway and GLI transcription factor, affected cells demonstrate cancerous phenotypes, including the proliferation of HCC cells, the epithelial-mesenchymal transition (EMT) process, and migration of HCC cells. In addition, a cancer stem cell marker observed apoptosis inhibition, increased cancer cell survival, and expression of CD133^[8,22].

Considering the importance of the SHH signaling pathway in carcinogenesis, several studies have been conducted with different approaches to inhibit this pathway at various levels of ligand, SMO regulatory factor, and GLI transcription factor on HCC tumor cells and other cancers. Given the key role of the SHH pathway and GLI transcription factor in the growth and progression of many cancers, especially HCC tumors, inhibition of this pathway has been considered for targeted control of cancer. In this regard, some studies have shown that targeted inhibition of this pathway leads to a reduction in cancerous phenotypes, such as high cell proliferation rate, migration, invasion, and angiogenesis, as well as the induction of apoptosis in the HCC cells and other cancers^[3,23-27].

Nucleic acid-based active biomolecules, representing a new class of potential bioactive medications, can induce/inhibit many molecular pathways. Many experimental and translational studies use biomolecules such as siRNA, miRNA, shRNA, *etc.*^[28-30].

Accordingly, researchers have developed an innovative targeted approach in cancer treatment using decoy oligodeoxynucleotide (ODN). Under normal circumstances, the transcription factor binds to a specific sequence (10-6 bp) in the promoter region of its target genes. This gene-protein binding sequence is specified for a transcription factor but may differ by several base pairs in the promoter regions of different genes. In this case, a canonical and common motif is defined for the correct binding of the transcription factor to its specific promoter. Decoy also has minimal effect on inactive transcription factors and normal cells, which is one of the strengths of this approach among other new treatment modalities^[31].

Decoy ODN is a short, double-stranded oligodeoxynucleotide whose sequence is designed based on the promoter sequence of the binding site of the target transcription factor. This oligodeoxynucleotide can be introduced into the cell by different methods. Decoy ODN aligns with the target transcription factor and inhibits the initiation of the transcription process^[32,33]. So far, various methods have been used to inhibit the SHH pathway in HCC cells. In this study, we used the specific decoy ODN to trap the GLI transcription factor in HCC cells, inhibiting the downstream target genes. It is demonstrated that using decoy ODN reduced the expression of GLI-downstream target genes and attenuated cancerous phenotypes.

MATERIALS AND METHODS

Cell culture

The HCC cell line, Huh-7, was obtained from the Royan Stem Cell Bank (Tehran, Iran). Huh-7 cells were cultivated in Dulbecco's modified Eagle's medium (DMEM)/high glucose (Gibco, 11960-044, US) supplemented with 10% fetal bovine serum (FBS, Gibco, 16140-071, US), 1% penicillin/streptomycin (Pen/Strep, Gibco, 15070-063, US), 1% L-glutamine (Gibco, 25030-024, US), and 1% minimum essential medium (MEM) non-essential amino acids (Gibco, 11140-035, US), at a temperature of 37 °C with 90% humidity and 5% CO₂.

GLI-specific decoy ODN

Twenty-Mer GLI-specific phosphorothioated decoy ODNs (GLI-specific decoy ODN) were designed based on the *IFITM5* human gene (Metabion AG, Germany). Sense and antisense strands (5'-CGCCTCGAGACCACTTGATC, GCGGAGCTCTGGTGAAGTAG-3') were dissolved in sterile Tris/EDTA buffer, annealed at 85 °C for 8 min, then cooled gradually to reach room temperature, and were finally stored at -20 °C.

Transfection procedure

The optimal ratio of DNA to transfection reagent was determined to be 1:2. The cationic lipid transfection reagent (X-tremeGENE HP DNA, Roche, Sigma-Aldrich, 06366236001, US) was used to transfect ODNs to the cells. GLI-specific decoy ODNs were also labeled by Cy3 fluorescent dye for intracellular tracking and transfection efficiency. GLI-specific decoy ODN and transfection reagent were mixed in a 96-well plate, and after 30 min of incubation, the complex was added to the cells in a dropwise manner. Transfections were carried out using FBS-free media. After 6 h of incubation, the medium of the cells was changed to a complete medium. All experiments were done and assayed 48 h after decoy transfection (post-transfection), except for transfection efficiency (at 6, 24, and 48 h post-transfection) and colony formation assay (14 days after transfection) [Supplementary Figure 1B]. For this study, we considered three experimental groups. The control group was Huh-7 cells that had not received any treatment. The next group consists of cells treated only with transfection reagents called the vehicle group. The treatment group is those who received GLI-specific decoy ODNs through transfection reagents. HCC cell lines (Hep-3B, HepG2, and Huh-7) were obtained from the Royan Stem Cell Bank at Royan Stem Cell Biology Institute, Tehran, Iran.

Dose escalation and cell viability

Cell viability was evaluated by the neutral red uptake assay (ab234039, Abcam, UK) in all three experimental groups (Control, Vehicle, and GLI-specific decoy ODN). First, 30×10^3 cells/well were seeded in 48-well plates and transfected by different concentrations of GLI-specific decoy ODN (450, 850, and 1250 nM). After 48 h, the medium was removed, and 2 µL of the neutral red solution (5 mg/mL) was added to each well and incubated at 37 °C for 40 min in dark conditions. Then, the media were removed and washed with phosphate-buffered saline (PBS). Afterward, 0.05 ml of acetic acid (100063, Sigma-Aldrich, US) solvent buffer was added to each well and incubated for another 20 min. Finally, the optical absorption of the wells was measured at a wavelength of 540 nm using an ELISA reader (Thermo Scientific).

Transfection efficiency

Huh-7 cells were grown in 4-well plates at a density of 6×10^5 cells/well. At the confluence of 70%, the cells were transfected with Cy3-labeled decoy ODNs (850 nM). The treated cells were observed at 6, 24, and 48 h. Nuclei of the cells were stained by 0.5 µL/well of Hoechst dye (B2261, Sigma-Aldrich, US) and washed with PBS. Intracellular cy3-labeled GLI-specific decoy ODN was tracked using fluorescent microscopy (Olympus IX71).

Gene expression analysis (quantitative RT-PCR)

Total RNA was isolated according to the manufacturer's protocol, Nucleospin[®] RNA II Kit (MN, 740955.50, Germany). In the reverse transcription reaction, cDNAs were synthesized from 1 µg of total purified mRNA with PrimeScript[™] 1st strand cDNA Synthesis Kit (Takara Bio, 6110A, Japan), according to the manufacturer's protocol. qRT-PCR was performed to evaluate mRNA expression levels in each sample with the SYBR Green master mix (Takara, RR820, Japan) and Step One Plus Real-time PCR System (Applied Biosystems, US). Initially, denaturation was performed at 95 °C for 10 min; then, the following thermal cycles were repeated 45 times: 95 °C for 30 s, 60 °C for 1 min, and 72 °C for 30 s. The average expression of the housekeeping gene was used to normalize the cDNA levels, and data analysis was performed by the comparative CT method ($2^{-\Delta\Delta C_t}$). The primer sequences used in this study are listed in [Table 1](#).

Cell proliferation (Bromodeoxyuridine incorporation assay)

Bromodeoxyuridine (BrdU) assay kit (11296736001, Roche, Sigma-Aldrich, US) was used to determine the potency of GLI-specific decoy ODN in inhibiting HCC cell proliferation. Huh-7 cells were plated on a 48-well plate 10^4 cells/well and then treated with the selected concentration of GLI-specific decoy ODN (850 nM). After 48 h of incubation, when the cells reached 50% confluency, BrdU labeling solution (10 mM, 200 µL/well) was added at 37 °C for 1 h; this was done according to the manufacturer's protocol. Cells were then fixed, washed, and stained. The nuclei were counterstained with DAPI (10 µg/mL, Sigma-Aldrich, D8417) for 15 min at room temperature. The average number of BrdU-positive cells was counted in 5-10 different high-power fields for each well and expressed as the percent of all cells. The fluorescent micrographs were captured using a fluorescent microscope (Olympus IX71).

Colony formation assay

The impact of GLI-specific decoy ODN on the colony-forming potency of Huh-7 cells was investigated in control, vehicle, and GLI-specific decoy ODN-treated groups. In the transfection procedure, Huh-7 cells were seeded at a density of 3.5×10^5 cells/well in a 6-well plate and transfected. After 24 h, adherent cells were harvested in all experimental groups, and single cells (700 cells/well) were plated in a 6-well plate. Then, the plated cells were incubated at 37 °C (with 90% humidity and 5% CO₂) and monitored for 14 days. The media exchange of each group (the decoy ODNs, reagents, and culture medium) was performed every four days. Colonies were fixed with 4% paraformaldehyde solution, stained with 0.2% crystal violet, and then imaged. In the next step, the total enumeration and surface area of the emerged colonies were automatically measured via the ImageJ 1.52a software.

Transwell[®] migration assay

Based on the following outlines [[Supplementary Figure 1B](#)], the Transwell[®] migration assay was performed in 24-well inserts (8.0 µm pore size; SPL, 36224, Korea). First, 5×10^5 cells/well of each group (GLI-specific decoy ODN, vehicle, and control) in a serum-free DMEM were plated and transfected in the top chamber inserts. Serum-enriched DMEM (10% FBS) was added to the lower chamber and incubated for 48 h. Then, the medium and the unmigrated cells were removed from the top chamber using cotton swabs and PBS. The migrated cells that had penetrated to the other side of the chamber were fixed with 70% Ethanol for 30 min and stained with a 0.2% crystal violet solution for 2 h. Eventually, the migrated cells were counted and imaged via a phase-contrast microscope (Olympus, IX71, Japan) in five random fields (magnification, $\times 100$).

Cell apoptosis assay

Cells were seeded into the 6-well plates (a density of 1.5×10^5 cells/well) and transfected for the cell

Table 1. List of the sequence of primers used for qRT-PCR

Target genes	Primers
<i>GAPDH</i> ¹	F: 5'-CTCATTTCCTGGTATGACAACGA-3' R: 5'-CTTCCTCTTGCTCTTGCT-3'
<i>c-MYC</i>	F: 5'-ACACATCAGCACAACACTACG-3' R: 5'-CGCCTCTTGACATTCTCC-3'
<i>SNAI2</i> ²	F: 5'-CGAACTGGACACACATACAGTG-3' R: 5'-CTGAGGATCTCTGGTTGTGGT-3'
<i>ZEB1</i> ³	F: 5'-TTCACAATTACTCACCTGTCCA-3' R: 5'-TGCCTCACATGTCTTTGATCTC-3'
<i>CDH4</i> ⁴	F: 5'-AATCACATCCTACACTGCC-3' R: 5'-GCAACTGGAGAACCATTGTC-3'
<i>CDH2</i> ⁵	F: 5'-AGCCAACCTTAACCTGAGGAGT-3' R: 5'-GGCAAGTTGATTGGAGGGATG-3'
<i>PROM1</i> ⁶ (CD133)	F: 5'-AGTCGGAACTGGCAGATAGC-3' R: 5'-GGTAGTGTGTACTGGCCAAT-3'

¹Glyceraldehyde 3-phosphate dehydrogenase; ²Glyceraldehyde 3-phosphate dehydrogenase; ³Glyceraldehyde 3-phosphate dehydrogenase; ⁴Glyceraldehyde 3-phosphate dehydrogenase; ⁵Glyceraldehyde 3-phosphate dehydrogenase; ⁶Glyceraldehyde 3-phosphate dehydrogenase.

apoptosis assay. After 48 h of transfection, all cells were collected via trypsinization and centrifuged at 4 °C for 5 min at 1,200 rpm. Then, the cells were stained with Annexin V and propidium iodide (APOAF, Sigma) according to the manufacturer's protocol. Cell apoptosis of all experimental groups was evaluated via flow cytometry (BD FACSCalibur), and data analysis was conducted by the FlowJo program (v.7 software).

Statistical analysis

All the data were analyzed using one-way ANOVA with GraphPad Prism 9.0 software. Data are reported as mean ± standard deviation (SD) for at least three independent biological experiments. The * $P \leq 0.05$, ** $P \leq 0.01$, *** $P \leq 0.001$, and **** $P \leq 0.0001$ values were considered statistically significant.

RESULTS

The activation of GLI is required for the survival of Huh-7 cells

To explore the connection between the SHH signaling pathway, EMT, stemness, and cell tumor growth, a protein-protein interaction (PPI) network was constructed using the STRING database. This network aimed to identify crucial hub genes associated with these functions. The collected data underwent purification, and network centrality parameters (specifically, betweenness, closeness, and eigenvector) were computed using Gephi-0.9.2 software. In silico data analysis revealed the pivotal role of GLI2 activation in SHH signaling, stemness genes, and EMT. The results announced that GLI2 exhibited the highest degrees of closeness centrality (0.69), betweenness (364.36), and eigenvector (0.84), establishing it as the most significant central hub protein within this PPI network [Figure 1A].

As shown in Figure 1B, the *GLI* gene's expression is higher in the Huh-7 cell line compared to the other examined hepatoma cell lines. A neutral red uptake assay was used to evaluate the effect of GLI-specific decoy ODN on Huh-7 cell viability. Our results demonstrated that a concentration of 850 nM GLI-specific decoy ODN entailed the most significant cell viability reduction ($56.36\% \pm 3\%$, **** $P \leq 0.0001$) in comparison to the other evaluated concentrations (450, 1,250 nM) [Figure 1C]. Therefore, we chose this concentration for the transfection of cells, and for the rest of the study, there was no significant difference between the control and vehicle groups.

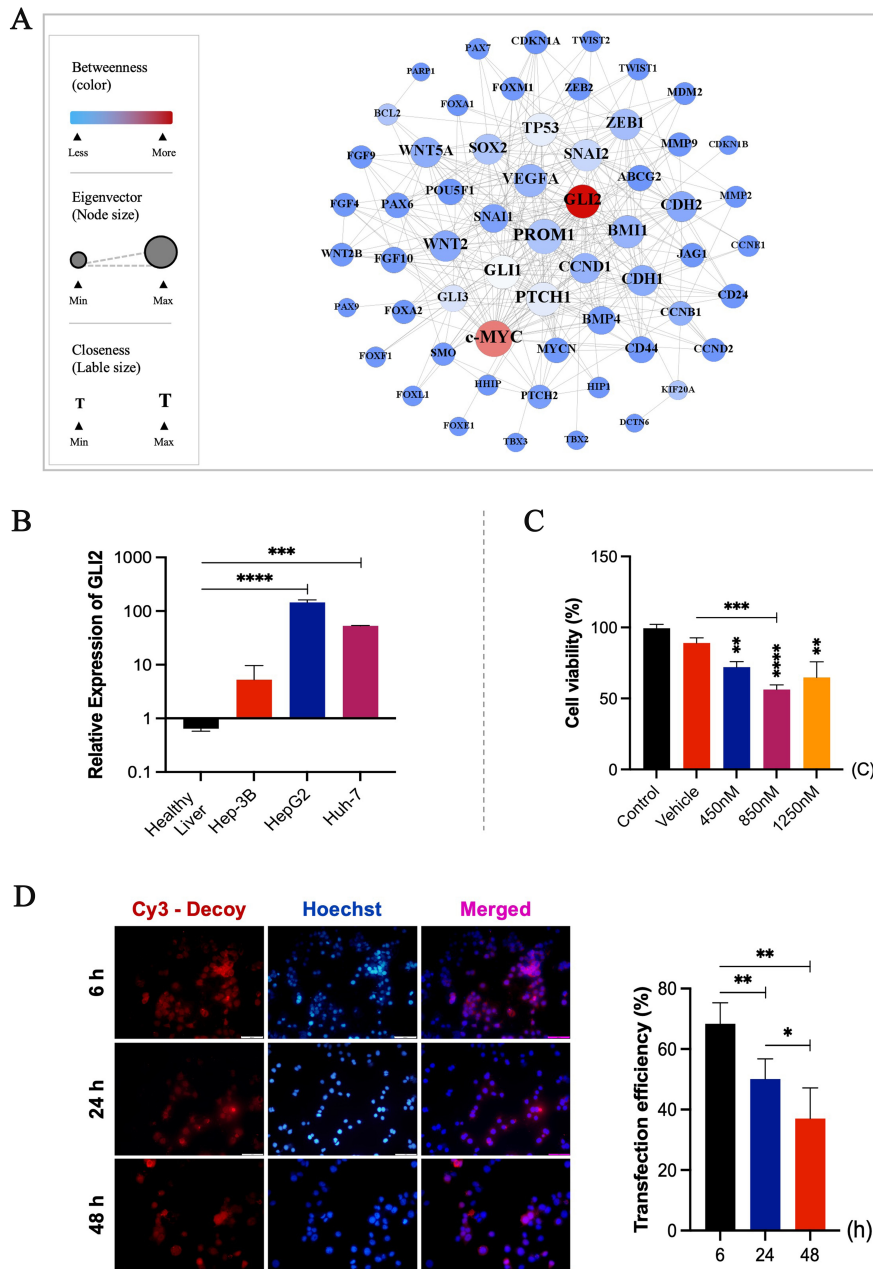


Figure 1. GLI activation is required for the survival of Huh-7 cells. (A) Protein-protein interaction network of the SHH signaling pathway, stemness, and EMT-involved proteins was obtained from the STRING database and purified by Gephi software. This network shows the importance of GLI2 and its connections with other proteins; (B) Quantifying mRNA expression levels of the *GLI2* gene involved in the SHH pathway were assessed in 3 available HCC cell lines (Hep-3B, HepG2, and Huh-7) and compared to healthy liver cells by qRT-PCR. Despite the remarkable expression of GLI in HepG2 and Huh7 cells, we selected Huh-7 cells for this study due to some technical concerns; (C) The impact of decoy ODN on the cell viability of Huh-7 cells was evaluated by the Neutral red uptake assay at three different concentrations (450, 850, and 1,250 nM). The optimum inhibitory effect of GLI-specific decoy ODN was on 850 nM (56.36% ± 3%) compared to control (99.39% ± 3%) and vehicle (89.08% ± 3%) groups (Vertical stars are representative of statistically significant data compared to the control group); (D) The transfection efficiency of 850 nM Cy3-decoy on Huh-7 cells at three different time points (6, 24, and 48 h) after transfection. Cy3-decoy was transfected to cells with X-tremeGENE HP DNA. GLI-specific decoy ODN and the nuclei of HuU7 cells were counterstained with Cy3-decoy and Hoechst, red and blue, respectively (scale bars, 100 μm). Quantification of transfected cells demonstrated the highest transfection efficiency at six hours post-transfection (68.38% ± 7%). Data are presented as the mean ± SD for three independent experiments. * $P \leq 0.05$, ** $P \leq 0.01$, *** $P \leq 0.001$, **** $P \leq 0.0001$. GLI: Glioma-associated oncogene; SHH: Sonic Hedgehog; EMT: epithelial-mesenchymal transition; HCC: hepatocellular carcinoma; ODN: oligodeoxynucleotides; SD: standard deviation.

Huh-7 cells were transfected with 850 nM Cy3-labeled decoy, and appropriate micrographs were taken during a 48-h period. The fluorescent micrographs [Figure 1D] indicated that after 6 h of transfection, about 68.38% ± 7% (** $P \leq 0.01$) of the cells were positive for Cy3-labeled decoy ODN. However, the transfected cell percentage reduced in a time-dependent manner, reaching 50.07% ± 6% after 24 h and 37.01% ± 10% after 48 h post-transfection.

GLI-specific decoy ODNs altered the expression pattern of GLI target genes and cell proliferation

To evaluate the effects of GLI-specific decoy ODN treatment on the expression levels of the GLI target genes, 48 h post-transfection, total RNAs of the three experimental groups were extracted. Following cDNA synthesis, the gene expression analysis was performed using qRT-PCR analysis [Figure 2A and B]. The transcripts for the stemness markers *PROM1* (CD133) and *c-MYC*, as well as the EMT markers *ZEB1* and *SNAI2*, dramatically decreased in the GLI-specific decoy ODN-treated cells compared to the control and vehicle groups [Figure 2A and B]. Moreover, considering the “cadherin switch” which is a hallmark of the EMT–MET shift, at the gene expression level, we found a significant upregulation in *CDH1* (E-cadherin) expression in the GLI-specific decoy ODN-treated group in comparison to the control group [Figure 2B]. Upregulation in *CDH2* (N-cadherin) expression also happened in the treated group.

Cell proliferation analysis of the Huh-7 cells was performed after 48 h of treatment with GLI-specific decoy ODNs. As represented in Figure 2C, the population of BrdU-positive cells in the GLI-specific decoy ODN-treated group significantly reduced compared to the control and vehicle ones (** $P \leq 0.01$).

GLI-specific decoy ODNs reduced the colony formation and migration capacity of the Huh-7 cell line

Concordant with the abovementioned results, colony formation assay showed that GLI-specific decoy ODN-treated cells noticeably impaired the colony formation potency of Huh-7 cells compared to the control and vehicle groups [Figure 3A]. As shown in Figure 3B, the mean area of colonies (pixel > 60, via ImageJ 1.52a software analysis) and surviving fraction's percentage of GLI-specific decoy ODN-treated group decreased significantly compared to the control and vehicle groups.

To validate whether the GLI-specific decoy ODN treatment of Huh-7 cells, in addition to reducing transcripts for *EMT* genes, could also affect their migration capacity, we used the Transwell migration assay [Figure 3C]. GLI-specific decoy ODN-treated cells showed significantly less cell migration potential through chamber membrane pores than the control and vehicle groups [Figure 3D].

GLI-specific decoy ODNs treatment induced apoptosis in Huh-7 cells

Evaluating cell apoptosis rate using annexin V and PI, we found a significant increase in early and late apoptotic cells following GLI-specific decoy ODN treatment compared to the control and vehicle groups [Figure 4A and B].

DISCUSSION

Hepatocellular carcinoma (HCC) is the most common liver malignancy and the second leading cause of cancer death worldwide^[4]. The current treatments for patients with HCC face many challenges, such as drug-induced toxicity and various side effects^[34]. Therefore, researchers are trying to replace the current therapeutic methods with alternative therapies.

Alcohol, aflatoxin, and hepatitis B and C viral infections are the main culprits of severe liver damage^[35,36]. Liver damage leads to dysfunction or disruption of signaling pathways, followed by the aberrant expression of genes related to cancer phenotypes, such as uncontrolled proliferation, aggressive invasion and metastasis

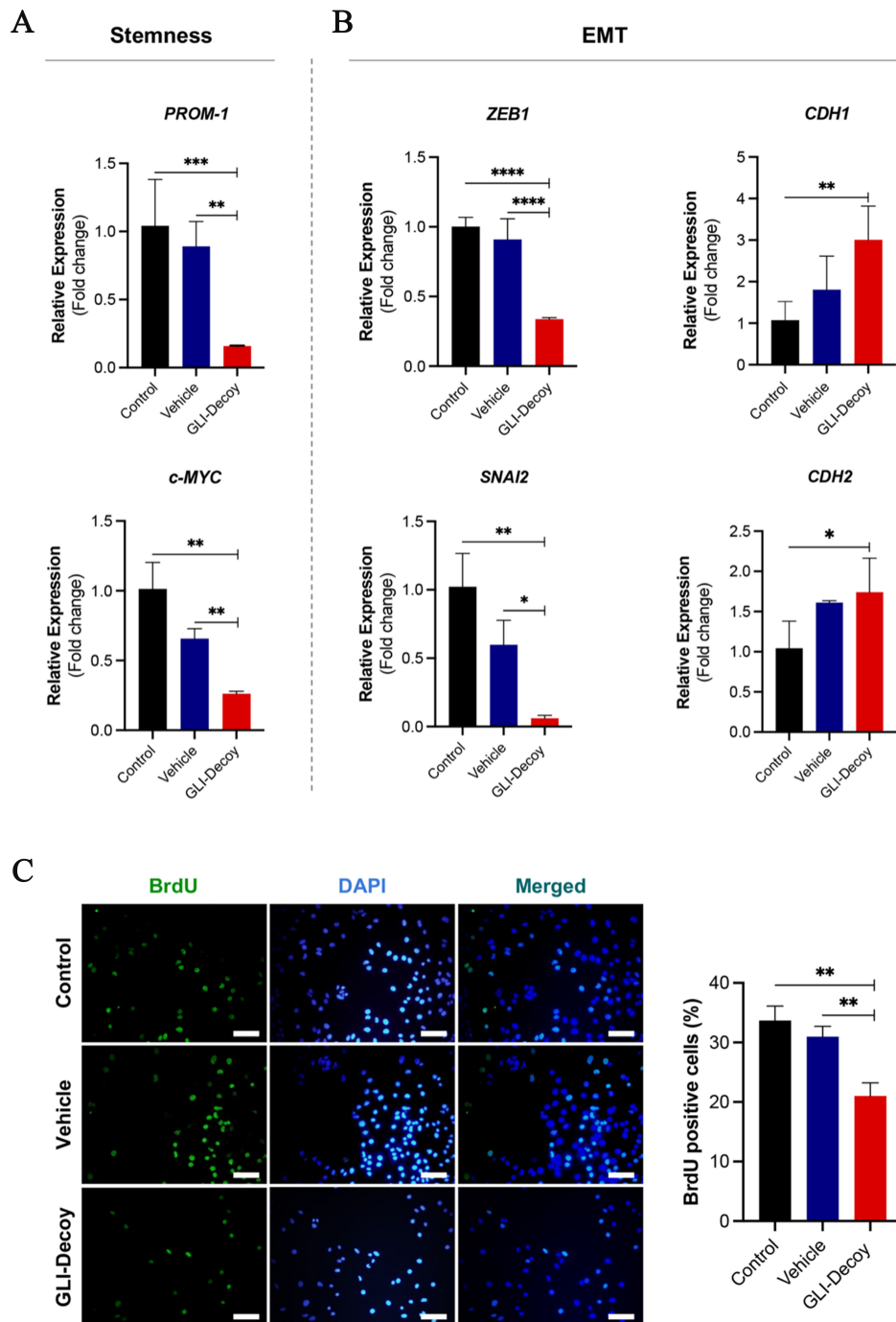


Figure 2. GLI-specific decoy ODN affects gene expression pattern and cell proliferation. (A and B) The GLI-decoy treatment significantly affected the transcripts of GLI-related genes associated with stemness and EMT in Huh-7 cells compared to the control and vehicle treatments; (C) GLI representative fluorescent micrographs and quantification of the BrdU assay demonstrated that in comparison to the control and the vehicle groups, cell proliferation of Huh-7 dramatically decreased following GLI-specific decoy ODN treatment. The BrdU-positive cells are green, and the nuclei in blue are counterstained with DAPI (scale bars, 100 μ m). Data are presented as the mean \pm SD for three independent experiments. * $P \leq 0.05$, ** $P \leq 0.01$, *** $P \leq 0.001$, **** $P \leq 0.0001$. GLI: Glioma-associated oncogene; ODN: oligodeoxynucleotides; EMT: epithelial-mesenchymal transition; BrdU: Bromodeoxyuridine; SD: standard deviation.

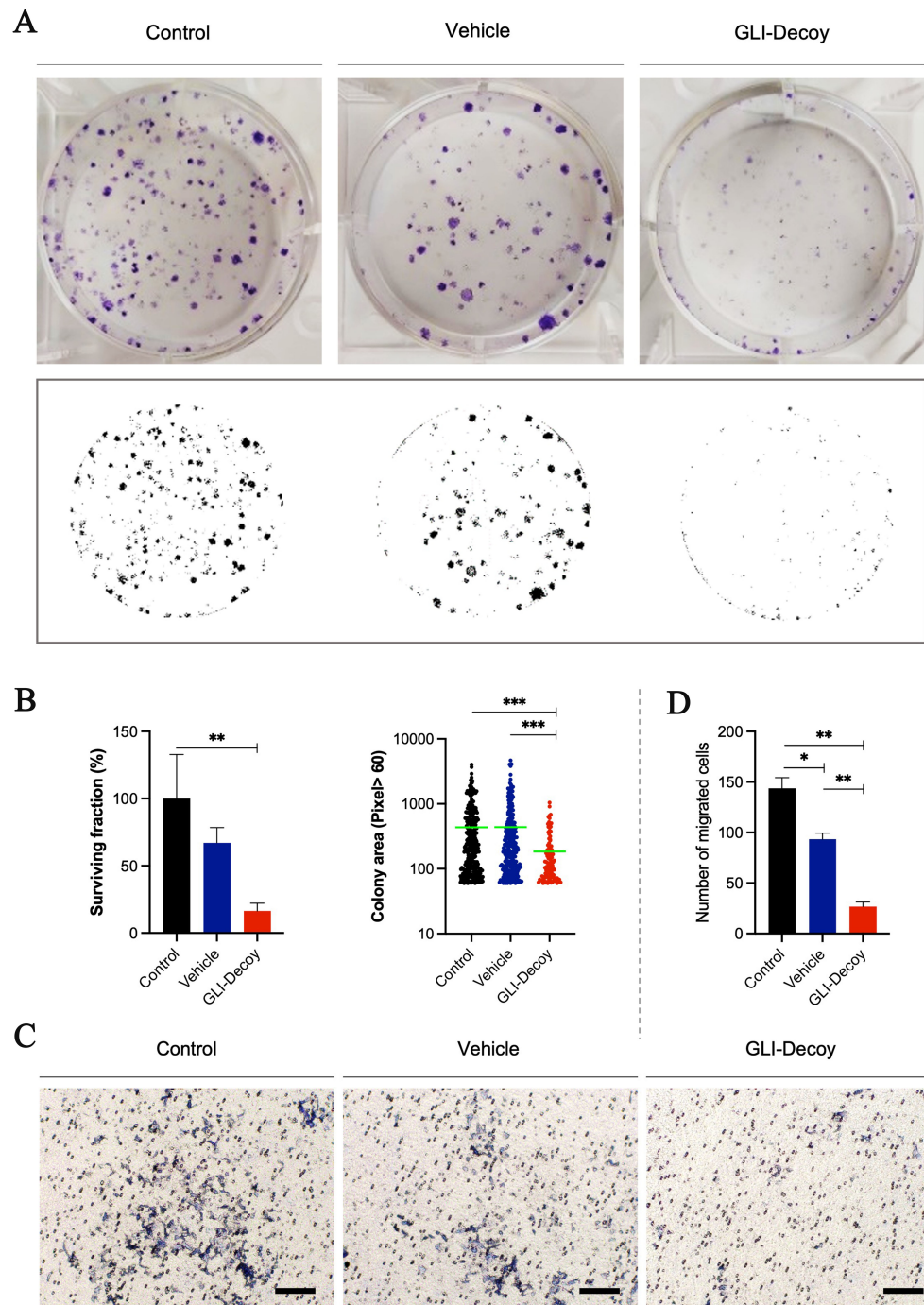


Figure 3. GLI-specific decoy ODN treatment decreased colony formation capacity and migration potential in the Huh-7 cell line. (A) The colony-formation assay indicated a significant reduction in the proliferative ability of Huh-7 cells after GLI-specific decoy ODN treatment. The same image as above after automatically identifying the wells via the ImageJ 1.52a software analysis. The image was converted into an 8-bit grayscale, and spaces between wells were removed using a mask; (B) The average area of colonies and the percentage of the surviving fraction decreased in treated Huh-7 cells compared to vehicle and control groups; (C) The Transwell® migration assay. (Scale bars, 100 µm); (D) To quantify the migration potential, the number of migrated cells was counted from five randomly selected fields under a phase-contrast microscope. Compared to the control and vehicle groups, the GLI-specific decoy ODN-treated group significantly reduced the number of migrated cells. * $P \leq 0.05$, ** $P \leq 0.01$, *** $P \leq 0.001$. GLI: Glioma-associated oncogene; ODN: oligodeoxynucleotides.

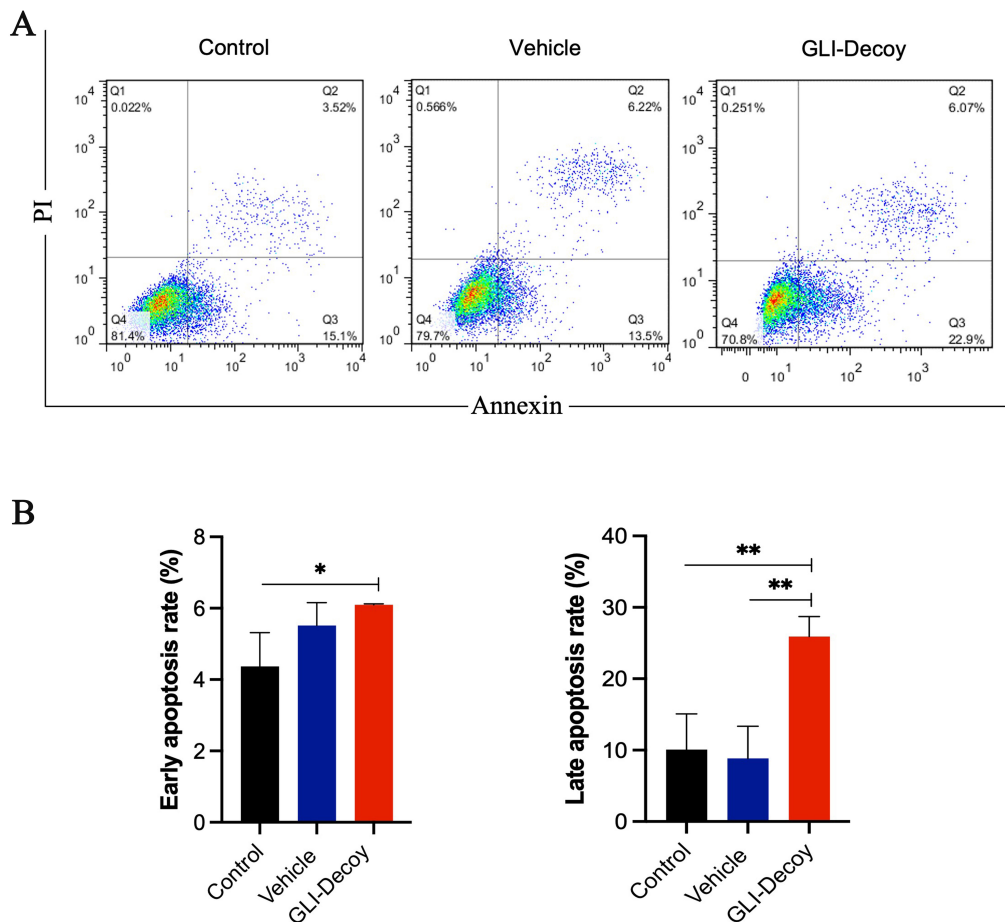


Figure 4. GLI-specific decoy ODN treatment induced apoptosis in the Huh-7 cell line. (A) The dot plots for flow cytometry analysis of apoptotic cells stained by annexin V/PI; (B) The apoptosis rate significantly increased in GLI-specific decoy ODN-treated cells compared to the control and vehicle groups (Early apoptosis: Control: 4.37%, Vehicle: 5.51%, GLI-decoy: 6.09%, Late apoptosis: Control: 10.09%, Vehicle: 8.85%, GLI-decoy: 25.9%). Data are presented as the mean \pm SD for three independent experiments. * $P \leq 0.05$, ** $P \leq 0.01$. GLI: Glioma-associated oncogene; ODN: oligodeoxynucleotides; SD: standard deviation.

of cancer cells, and apoptosis inhibition^[3,19,37]. Specific signaling pathways are activated in cancer cells to facilitate their survival in harsh conditions and promote tumor progression^[38]. Therefore, inhibiting the critical signaling pathways and targeting their essential components may offer novel cancer treatments^[39]. Unlike in healthy hepatocytes, the SHH signaling pathway is one of the most critical pathways activated in liver cancer cells^[9]. In addition, this signaling pathway has several crosstalks with other pathways, particularly with Notch, Wnt, TGF- β , and mTOR/S6K1^[8,10,40,41]. GLI transcription factor is activated in the SHH pathway and induces the genes associated with cancer phenotypes^[8,13].

According to some studies, using the decoy ODN method suppresses the function of specific transcription factors as a central component in the signaling pathways and selectively regulates, modifies, or inhibits the expression of downstream genes and their linked phenotypes^[33,42-46]. Considering the importance of the SHH signaling pathway in carcinogenesis^[3,23-26,28-30] and based on the effective results of applying the decoy ODN strategy^[33,42,46-48] in previous research, this study was formed.

We acknowledge the heterogeneity of cancer cells in HCC. The three most frequently used cell lines are Hep3B, HepG2, and Huh-7. However, we decided to use Huh-7 cells in our study because they primarily represent the features of adult HCC and are known as the most well-differentiated hepatic cancer cells. Indeed, Huh-7 cells were taken from a liver tumor mass of a 57-year-old Japanese male. These cells are highly heterogeneous and display a point mutation in the *p53* gene.

In contrast, Hep3B cells were isolated from a pediatric 8-year-old black male from the US, containing integrated Hepatitis B virus genome, and they are *p53* deficient cells. Furthermore, HepG2 cells of hepatoblastoma origin were isolated from liver biopsy specimens of a 15-year-old Caucasian male from Argentina with primary hepatoblastoma and are known to be wild-type *p53*^[34]. Huh-7 cells are well-differentiated cancer cells. This cell line is a tumorigenic cell line with epithelial characteristics and shows little invasive behavior^[49]. On the other hand, we quantified the relative expression of the *GLI* gene in three widely used HCC cell lines [Figure 1B]. Despite the remarkable expression of *GLI* in HepG2 and Huh-7 cells, we selected Huh-7 cells for this study due to some technical concerns. The HepG2 cell line was not chosen due to technical issues such as being hard to transfect, handle, and manipulate. Huh-7 cells are highly differentiated cancer cells. In the current study, comparing three HCC cell lines, we chose Huh-7 for further experiments on the SHH signaling pathway.

Most transcription factors can have a significant impact on the gene expression profile with small changes in their concentrations because transcription factors are located at the top of the cell's gene expression cascade. So far, various methods have been used to target Shh pathway inhibition in HCC, including (1) Small Molecules, (2) Herbal extracts, and (3) RNA-based biomolecules. The results showed that the targeted inhibition of this pathway is associated with the reduction of cancerous phenotype in HCC and other cancers^[23,24,28,30,50,51]. Decoy inhibits specific transcription factors in the pre-transcription stage and the expression of genes involved in cancer initiation. Decoy also has a minimal effect on inactive transcription factors and normal cells, which is one of the strengths of this approach among targeted therapy options. The mentioned studies showed a remarkable reduction of angiogenesis, inhibition of cell growth and proliferation, and increase in apoptosis rate in cancer cells treated with decoy ODN^[33,42,52,53].

Our approach was to apply *GLI*-specific decoy ODN to inhibit activated *GLI* transcription factors in the HCC cell line at the pre-transcriptional phase. Therefore, the main aim of this study was to use the decoy ODN method to inhibit the function of *GLI* transcription factor in the HCC cells to alter their cancerous phenotype in terms of cell proliferation, colony formation, EMT, cell migration, and apoptosis.

At first, we performed a bioinformatics analysis and found *GLI2* is the central hub protein in the SHH signaling pathway with a high impact on EMT and cell tumor growth. Therefore, we designed the *GLI*-specific decoy ODN. Then, based on cell viability data and applying the Cy3-decoy test, we found the effective dose and the transfection efficiency are 850 nM ($56.36\% \pm 3\%$, $****P \leq 0.0001$) and 6 h after transfection ($68.38\% \pm 7\%$, $**P \leq 0.01$). The results of the BrdU test indicated a significant decrease in cell proliferation rate in the Huh-7 cells treated with *GLI*-specific decoy ODN. Quantitative RT-PCR data showed that the *c-MYC* gene's expression decreased in the group treated with *GLI*-specific decoy ODN. In line with the previous lung and breast cancer studies, decoy ODN has a considerable influence on reducing the proliferation rate of cancer cells^[33,48].

The reduction in the expression level of *PROM1*, a critical cancer stem cell marker (CD133), was shown by qRT-PCR analysis. By performing the colony formation test, we also evaluated and measured the survival rate of cells and their capacity for proliferation and colonization. Similar findings were achieved in 2010 in

patients with osteosarcoma^[30], in 2019 in liver cancer^[25], and in 2020 in HCC patient-derived organoid (PDO) models^[24] on the colonization ability of cancer cells after inhibiting GLI and SMO by some small molecules. The results of our research are consistent with the results obtained in the mentioned articles, and the colonization capacity in the cells treated with decoy has decreased significantly ($P \leq 0.01$).

Previous studies showed that by inhibiting GLI transcription factors with the assistance of various types of small molecules (such as GANT61 and 5-FU), cell migration was reduced in HCC cells^[24,27]. In 2020, Johari *et al.* also reported the reduction of cell migration with the decoy ODN strategy in breast cancer^[45]. In this study, Transwell' assay was used to investigate cell migration. Our results were consistent with the reports mentioned above. Our findings indicated a decreasing expression of mesenchymal genes (including *ZEB1* and *SNAI2*) and a conversely increasing expression of the epithelial gene (*CDH1*) at molecular analysis. Although the expression status of *CDH1* remarkably met the "cadherin switch", the expression of *CDH2* was not in line with what we expected [Figure 2A and B].

An annexin V/PI kit was used for flow cytometry analysis to evaluate cell death. Targeting various components of the SHH pathway resulted in apoptosis induction, as shown in multiple cancers, including HCC; our results align with these studies^[25,29].

In addition, some studies have shown decoy's efficiency in animal models. Zhang *et al.* (2007) conducted a study to limit the excessive activity of STAT3 in human lung cancer cells^[48]. In this experiment, the effects of STAT3 decoy ODN were investigated *in vitro* (cell line A549) and *in vivo* (xenograft of a nude mouse carrying a lung carcinoma tumor). In addition, STAT3 decoy ODN inhibited lung tumor growth in the mouse model and decreased the expression of *bcl-xl* and *cyclin D1* genes. According to this research, STAT3 decoy ODN was able to significantly suppress lung cancer cells in both *in vitro* and *in vivo* conditions; therefore, it can be considered a potential therapeutic method for treating lung cancer^[48].

In a study published in the journal *Cancers* this year (5 April 2024), the role of SHH signaling in the resistance of HCC to chemotherapy, target therapy, and radiation therapy was investigated in detail. SHH ligands are identified in approximately 60% of HCC tumor cells. At the same time, GLI2 is found in over 84% of HCC cells^[54].

In another study, higher levels of GLI2 protein expression in HCC cells compared to normal liver were determined by immunohistochemical staining. The analysis revealed that patients with GLI2 overexpression had significantly shorter overall survival. This case was significantly associated with tumor differentiation, vascular invasion, early recurrence, and intra-hepatic metastasis^[55].

We have investigated using decoy strategy for the first time in the present study. Miroslava Didiysova *et al.* provided a beneficial review article that discussed the contribution of Hh signaling crosstalk with other pro-tumorigenic pathways and presented GLIs as the central hubs in tumor signaling networks^[56].

In 2006, Edifiligid was the first decoy to target the cell cycle regulator E2F. It is considered the first decoy investigated in humans, but it did not have clinical efficacy^[57].

In 2011, the first report of intra-tumoral injection of a STAT3 decoy ODN in head and neck squamous cell carcinoma patients was published. This study showed the effects of repressors on the expression of the STAT3 target gene^[58]. Among the decoys that have had successful results *in vitro*, only NFkB and STAT3 have entered clinical trials^[59,60].

Although no study has been conducted to investigate the performance of GLI-decoy in *in vivo* studies, the application of GLI-specific decoy ODN in *in vivo* experiments could result in off-target effects since SHH signaling is an important signaling pathway in many cells. To avoid any possible off-target effects, targeted delivery to the particular organ could be a solution in preclinical and future clinical studies.

We propose some ideas for future research: (1) Simultaneous application of GLI decoy and other specific decoys of important transcription factors in HCC such as STAT and NF- κ B; (2) Investigating this approach in other HCC cell lines using a scrambled decoy ODN; (3) Investigating the anticancer effects of GLI decoy in animal models (*in vivo*); (4) Evaluation of combination therapy: using the oligodeoxynucleotide decoy method along with small molecules or other biomolecules that can change cancerous phenotypes; (5) Use of oligodeoxynucleotide decoy method as a pretreatment method before surgery and radiotherapy.

Notably, previous studies have consistently highlighted the limited activity of the SHH pathway in healthy hepatocytes^[9,10]. Therefore, targeting and inhibiting this pathway could be a potential strategy to restore healthy status in cancerous cells. In addition, this idea further supports its potential effectiveness in selectively targeting cancer cells and reducing the risk of off-target.

One limitation of our research is the lack of a non-specific ODN. This could have offered valuable insights into the specificity of the decoy ODNs utilized in our experiments. The incorporation of a scramble group would have enabled us to differentiate between the impacts of the decoy ODNs and any incidental non-specific interactions that may have taken place. However, due to some limitations, we were unable to include this control group. This oversight will be addressed in future studies, where we plan to incorporate a scramble group to further validate our findings and ensure that the observed effects are specific to the GLI pathway.

In conclusion, based on the results from this study and previous studies, the SHH signaling pathway could be a potential molecular target in cancer treatment research. This study's results have indicated that treatment with a dose of 850 nM GLI-specific decoy ODN significantly reduces cancerous phenotypes in Huh-7 cells in terms of cell proliferation, cell migration, EMT, and colony formation, as well as inducing apoptosis.

DECLARATIONS

Acknowledgments

The authors would like to express their gratitude to the supporting colleagues at Royan Institute (Tehran, Iran). During the preparation of this work, the authors used [BioRender](#) to create the graphical abstract.

Author contributions

Performed the assays *in vitro*: Hajilou Z

Analyzed the data: Heydari Z, Solhi R, Torabi S, Bahadori S, Vosough M

Interpreted the data and wrote the manuscript: Heydari Z, Solhi R, Nussler AK, Vosough M

Designed this study: Hajilou Z, Solhi R, Farzaneh Z, Vosough M

Revised the paper: Nussler AK, Vosough M, Hassan M, Piryaee A, Solhi R, Shokouhian B

Financially supported the project: Vosough M

Carried out the final approval: Vosough M, Nussler AK

All authors have read and approved the final manuscript.

Availability of data and materials

The datasets generated during and/or analyzed during the current study are available from the corresponding authors upon reasonable request.

Financial support and sponsorship

This project was financially supported by grants from the Royan Institute (97000205) and Bahar Tashkhis Teb Co. (BTT, 9703, 9809, and 9903).

Conflicts of interest

All authors declared that there are no conflicts of interest.

Ethical approval and consent to participate

This study was approved by Royan Institute ethical committee and registered under the number: IR.ACECR.ROYAN.REC.1400.007.

Consent for publication

Not applicable.

Copyright

© The Author(s) 2024.

REFERENCES

1. Miri-Lavasani Z, Torabi S, Solhi R, et al. Conjugated linoleic acid treatment attenuates cancerous features in hepatocellular carcinoma cells. *Stem Cells Int* 2022;2022:1850305. DOI PubMed PMC
2. Shokouhian B, Negahdari B, Heydari Z, et al. HNF4 α is possibly the missing link between epithelial-mesenchymal transition and Warburg effect during hepatocarcinogenesis. *Cancer Sci* 2023;114:1337-52. DOI PubMed PMC
3. Jeng KS, Jeng CJ, Jeng WJ, et al. Sonic Hedgehog signaling pathway as a potential target to inhibit the progression of hepatocellular carcinoma. *Oncol Lett* 2019;18:4377-84. DOI PubMed PMC
4. WHO. Data visualization tools for exploring the global cancer burden in 2022. Available from: https://gco.iarc.fr/today/online-analysis-pie?v=2020&mode=cancer&mode_population=continents&population=900&populations=900&key=total&sex=0&cancer=39&type=1&statistic=5&prevalence=0&population_group=0&ages_group%5B%5D=0&ages_group%5B%5D=17&nb_items=7&group_cancer=0&include_nmssc=0&include_nmssc_other=1&half_pie=0&donut=0. [Last accessed on 28 Jul 2024].
5. Suresh D, Srinivas AN, Kumar DP. Etiology of hepatocellular carcinoma: special focus on fatty liver disease. *Front Oncol* 2020;10:601710. DOI PubMed PMC
6. Aasadollahei N, Rezaei N, Golroo R, Agarwal T, Vosough M, Piryaei A. Bioengineering liver microtissues for modeling non-alcoholic fatty liver disease. *EXCLI J* 2023;22:367-91. DOI PubMed PMC
7. Whittaker S, Marais R, Zhu AX. The role of signaling pathways in the development and treatment of hepatocellular carcinoma. *Oncogene* 2010;29:4989-5005. DOI PubMed
8. Carballo GB, Honorato JR, de Lopes GPF, Spohr TCLSE. A highlight on Sonic hedgehog pathway. *Cell Commun Signal* 2018;16:11. DOI PubMed PMC
9. Della Corte CM, Viscardi G, Papaccio F, et al. Implication of the Hedgehog pathway in hepatocellular carcinoma. *World J Gastroenterol* 2017;23:4330-40. DOI PubMed PMC
10. Skoda AM, Simovic D, Karin V, Kardum V, Vranic S, Serman L. The role of the Hedgehog signaling pathway in cancer: a comprehensive review. *Bosn J Basic Med Sci* 2018;18:8-20. DOI PubMed PMC
11. Zheng X, Zeng W, Gai X, et al. Role of the Hedgehog pathway in hepatocellular carcinoma (review). *Oncol Rep* 2013;30:2020-6. DOI PubMed
12. Omenetti A, Choi S, Michelotti G, Diehl AM. Hedgehog signaling in the liver. *J Hepatol* 2011;54:366-73. DOI PubMed PMC
13. Gao L, Zhang Z, Zhang P, Yu M, Yang T. Role of canonical Hedgehog signaling pathway in liver. *Int J Biol Sci* 2018;14:1636-44. DOI PubMed PMC
14. Filgueira NA. Hepatocellular carcinoma recurrence after liver transplantation: risk factors, screening and clinical presentation. *World J Hepatol* 2019;11:261-72. DOI PubMed PMC
15. Shokouhian B, Aboulkheyr Es H, Negahdari B, et al. Hepatogenesis and hepatocarcinogenesis: alignment of the main signaling pathways. *J Cell Physiol* 2022;237:3984-4000. DOI
16. Fernandes-Silva H, Correia-Pinto J, Moura RS. Canonical sonic hedgehog signaling in early lung development. *J Dev Biol* 2017;5:3.

[DOI PubMed PMC](#)

17. Niewiadomski P, Niedziółka SM, Markiewicz L, Uśpieński T, Baran B, Chojnowska K. Gli proteins: regulation in development and cancer. *Cells* 2019;8:147. [DOI PubMed PMC](#)
18. Sabol M, Trnski D, Musani V, Ozretić P, Levanat S. Role of GLI transcription factors in pathogenesis and their potential as new therapeutic targets. *Int J Mol Sci* 2018;19:2562. [DOI PubMed PMC](#)
19. Machado MV, Diehl AM. Hedgehog signalling in liver pathophysiology. *J Hepatol* 2018;68:550-62. [DOI PubMed PMC](#)
20. Jeng KS, Sheen IS, Jeng WJ, et al. High expression of patched homolog-1 messenger RNA and glioma-associated oncogene-1 messenger RNA of sonic hedgehog signaling pathway indicates a risk of postresection recurrence of hepatocellular carcinoma. *Ann Surg Oncol* 2013;20:464-73. [DOI](#)
21. Dugum M, Hanouneh I, McIntyre T, et al. Sonic hedgehog signaling in hepatocellular carcinoma: a pilot study. *Mol Clin Oncol* 2016;4:369-74. [DOI PubMed PMC](#)
22. Shi C, Huang D, Lu N, et al. Aberrantly activated Gli2-KIF20A axis is crucial for growth of hepatocellular carcinoma and predicts poor prognosis. *Oncotarget* 2016;7:26206-19. [DOI PubMed PMC](#)
23. Harada K, Ohashi R, Naito K, Kanki K. Hedgehog signal inhibitor GANT61 inhibits the malignant behavior of undifferentiated hepatocellular carcinoma cells by targeting non-canonical GLI signaling. *Int J Mol Sci* 2020;21:3126. [DOI PubMed PMC](#)
24. Wang S, Wang Y, Xun X, et al. Hedgehog signaling promotes sorafenib resistance in hepatocellular carcinoma patient-derived organoids. *J Exp Clin Cancer Res* 2020;39:22. [DOI PubMed PMC](#)
25. Li J, Cai H, Li H, et al. Combined inhibition of sonic Hedgehog signaling and histone deacetylase is an effective treatment for liver cancer. *Oncol Rep* 2019;41:1991-7. [DOI PubMed](#)
26. Pinter M, Sieghart W, Schmid M, et al. Hedgehog inhibition reduces angiogenesis by downregulation of tumoral VEGF-A expression in hepatocellular carcinoma. *United European Gastroenterol J* 2013;1:265-75. [DOI PubMed PMC](#)
27. Wang Q, Huang S, Yang L, et al. Down-regulation of Sonic hedgehog signaling pathway activity is involved in 5-fluorouracil-induced apoptosis and motility inhibition in Hep3B cells. *Acta Biochim Biophys Sin* 2008;40:819-29. [PubMed](#)
28. de la Rosa J, Sánchez M, Enguita-Germán M, et al. Inhibition of the sonic hedgehog pathway by cyclopamine or GLI1 siRNA reduces *in vivo* tumorigenesis of human medulloblastoma cells xenotransplanted to immunodeficient nude mice. *Adv Transl Med Res* 2017;1:1-5. [DOI](#)
29. Du W, Liu X, Chen L, et al. Targeting the SMO oncogene by miR-326 inhibits glioma biological behaviors and stemness. *Neuro Oncol* 2015;17:243-53. [DOI PubMed PMC](#)
30. Hirotsu M, Setoguchi T, Sasaki H, et al. Smoothed as a new therapeutic target for human osteosarcoma. *Mol Cancer* 2010;9:5. [DOI PubMed PMC](#)
31. Leong PL, Andrews GA, Johnson DE, et al. Targeted inhibition of Stat3 with a decoy oligonucleotide abrogates head and neck cancer cell growth. *Proc Natl Acad Sci U S A* 2003;100:4138-43. [DOI PubMed PMC](#)
32. Youn SW, Park KK. Small-nucleic-acid-based therapeutic strategy targeting the transcription factors regulating the vascular inflammation, remodeling and fibrosis in atherosclerosis. *Int J Mol Sci* 2015;16:11804-33. [DOI PubMed PMC](#)
33. Rahmati M, Johari B, Kadivar M, Rismani E, Mortazavi Y. Suppressing the metastatic properties of the breast cancer cells using STAT3 decoy oligodeoxynucleotides: a promising approach for eradication of cancer cells by differentiation therapy. *J Cell Physiol* 2020;235:5429-44. [DOI PubMed](#)
34. Lin A, Giuliano CJ, Palladino A, et al. Off-target toxicity is a common mechanism of action of cancer drugs undergoing clinical trials. *Sci Transl Med* 2019;11:eaaw8412. [DOI PubMed PMC](#)
35. Kanda T, Goto T, Hirotsu Y, Moriyama M, Omata M. Molecular mechanisms driving progression of liver cirrhosis towards hepatocellular carcinoma in chronic hepatitis B and C infections: a review. *Int J Mol Sci* 2019;20:1358. [DOI PubMed PMC](#)
36. Sia D, Villanueva A, Friedman SL, Llovet JM. Liver cancer cell of origin, molecular class, and effects on patient prognosis. *Gastroenterology* 2017;152:745-61. [DOI PubMed](#)
37. Dongre A, Weinberg RA. New insights into the mechanisms of epithelial-mesenchymal transition and implications for cancer. *Nat Rev Mol Cell Biol* 2019;20:69-84. [DOI PubMed](#)
38. Ferlier T, Coulouarn C. Regulation of gene expression in cancer-an overview. *Cells* 2022;11:4058. [DOI PubMed PMC](#)
39. Villanueva A. Hepatocellular carcinoma. Reply. *N Engl J Med* 2019;381:e2. [DOI PubMed](#)
40. Farzaneh Z, Vosough M, Agarwal T, Farzaneh M. Critical signaling pathways governing hepatocellular carcinoma behavior; small molecule-based approaches. *Cancer Cell Int* 2021;21:208. [DOI PubMed PMC](#)
41. Wang Y, Ding Q, Yen CJ, et al. The crosstalk of mTOR/S6K1 and Hedgehog pathways. *Cancer Cell* 2012;21:374-87. [DOI PubMed PMC](#)
42. Han Q, Wang Y, Pang M, Zhang J. STAT3-blocked whole-cell hepatoma vaccine induces cellular and humoral immune response against HCC. *J Exp Clin Cancer Res* 2017;36:156. [DOI PubMed PMC](#)
43. Johari B, Rezaeejam H, Moradi M, et al. Increasing the colon cancer cells sensitivity toward radiation therapy via application of Oct4-Sox2 complex decoy oligodeoxynucleotides. *Mol Biol Rep* 2020;47:6793-805. [DOI PubMed](#)
44. Asadi Z, Fathi M, Rismani E, Bigdelou Z, Johari B. Application of decoy oligodeoxynucleotides strategy for inhibition of cell growth and reduction of metastatic properties in nonresistant and erlotinib-resistant SW480 cell line. *Cell Biol Int* 2021;45:1001-14. [DOI PubMed](#)
45. Johari B, Rahmati M, Nasehi L, Mortazavi Y, Faghfoori MH, Rezaeejam H. Evaluation of STAT3 decoy oligodeoxynucleotides'

- synergistic effects on radiation and/or chemotherapy in metastatic breast cancer cell line. *Cell Biol Int* 2020;44:2499-511. DOI PubMed
46. Geiger JL, Grandis JR, Bauman JE. The STAT3 pathway as a therapeutic target in head and neck cancer: barriers and innovations. *Oral Oncol* 2016;56:84-92. DOI PubMed PMC
 47. Nishimura A, Akeda K, Matsubara T, et al. Transfection of NF- κ B decoy oligodeoxynucleotide suppresses pulmonary metastasis by murine osteosarcoma. *Cancer Gene Ther* 2011;18:250-9. DOI PubMed
 48. Zhang X, Zhang J, Wang L, Wei H, Tian Z. Therapeutic effects of STAT3 decoy oligodeoxynucleotide on human lung cancer in xenograft mice. *BMC Cancer* 2007;7:149. DOI PubMed PMC
 49. Nwosu ZC, Battello N, Rothley M, et al. Liver cancer cell lines distinctly mimic the metabolic gene expression pattern of the corresponding human tumours. *J Exp Clin Cancer Res* 2018;37:211. DOI PubMed PMC
 50. Chen X, Cheng Q, She M, et al. Expression of sonic hedgehog signaling components in hepatocellular carcinoma and cyclopamine-induced apoptosis through Bcl-2 downregulation *in vitro*. *Arch Med Res* 2010;41:315-23. DOI PubMed
 51. Tang SN, Fu J, Nall D, Rodova M, Shankar S, Srivastava RK. Inhibition of sonic hedgehog pathway and pluripotency maintaining factors regulate human pancreatic cancer stem cell characteristics. *Int J Cancer* 2012;131:30-40. DOI PubMed PMC
 52. Sun X, Zhang J, Wang L, Tian Z. Growth inhibition of human hepatocellular carcinoma cells by blocking STAT3 activation with decoy-ODN. *Cancer Lett* 2008;262:201-13. DOI PubMed
 53. Kawamura I, Morishita R, Tsujimoto S, et al. Intravenous injection of oligodeoxynucleotides to the NF-kappaB binding site inhibits hepatic metastasis of M5076 reticulosarcoma in mice. *Gene Ther* 2001;8:905-12. DOI PubMed
 54. Jeng KS, Chang CF, Tsang YM, Sheen IS, Jeng CJ. Reappraisal of the roles of the sonic hedgehog signaling pathway in hepatocellular carcinoma. *Cancers* 2024;16:1739. DOI PubMed PMC
 55. Zhang D, Cao L, Li Y, Lu H, Yang X, Xue P. Expression of glioma-associated oncogene 2 (Gli 2) is correlated with poor prognosis in patients with hepatocellular carcinoma undergoing hepatectomy. *World J Surg Oncol* 2013;11:25. DOI PubMed PMC
 56. Didiasova M, Schaefer L, Wygrecka M. Targeting GLI transcription factors in cancer. *Molecules* 2018;23:1003. DOI PubMed PMC
 57. Tomita T, Kunugiza Y, Tomita N, et al. E2F decoy oligodeoxynucleotide ameliorates cartilage invasion by infiltrating synovium derived from rheumatoid arthritis. *Int J Mol Med* 2006;18:257-65. PubMed
 58. Sen M, Thomas SM, Kim S, et al. First-in-human trial of a STAT3 decoy oligonucleotide in head and neck tumors: implications for cancer therapy. *Cancer Discov* 2012;2:694-705. DOI PubMed PMC
 59. Hecker M, Wagner AH. Transcription factor decoy technology: a therapeutic update. *Biochem Pharmacol* 2017;144:29-34. DOI PubMed
 60. Mahjoubin-Tehran M, Teng Y, Jalili A, Aghaee-Bakhtiari SH, Markin AM, Sahebkar A. Decoy technology as a promising therapeutic tool for atherosclerosis. *Int J Mol Sci* 2021;22:4420. DOI PubMed PMC